Incommensurate matrix product state for quantum spin systems

Hiroshi Ueda[1,*] and Isao Maruyama[2,†]

[1]*Condensed Matter Theory Laboratory, RIKEN, Wako, Saitama 351-0198, Japan*

[2]*Graduate School of Engineering Science, Osaka University, Toyonaka, Osaka 560-8531, Japan*

(Received 9 May 2012; revised manuscript received 4 July 2012; published 27 August 2012)

We introduce a matrix product state (MPS) with an incommensurate periodicity by applying the spin-rotation operator of each site to a uniform MPS in the thermodynamic limit. The relation between the improvement of the variational method due to the spin-rotation operators and the spontaneous symmetry breaking of the MPS is studied. The optimized pitch of the rotational operator reflects the commensurate/incommensurate properties of spin-spin correlation functions in the $S = 1/2$ Heisenberg chain and the $S = 1/2$ ferromagnetic-antiferromagnetic zigzag chain.

DOI: 10.1103/PhysRevB.86.064438 PACS number(s): 75.10.Jm, 75.40.Mg

I. INTRODUCTION

An analysis of low-dimensional frustrated quantum spin systems beyond the mean-field approximation (MFA) is one of the attractive topics in quantum mechanics because rich quantum phases can appear due to the coexistence of frustration and strong quantum fluctuations. A typical example is the spin $S = 1/2$ ferromagnetic-antiferromagnetic (FM-AFM) zigzag Heisenberg/XXZ spin chain as a theoretical model of quasi-one-dimensional edge-sharing cuprates. In theoretical studies on this quantum Hamiltonian,[1–8] the exact diagonalization method (ED), the density-matrix renormalization-group method (DMRG),[9–12] and the infinite time-evolving block-decimation method (iTEBD)[13] were used as powerful methods in order to determine novel quantum phases.

In the DMRG and the iTEBD methods, variational states take the form of a matrix product state (MPS)[14–16] and an infinite MPS (iMPS),[13] respectively. When the dimension of the matrices constructing the MPS is 1, the MPS corresponds to the MFA. As the dimension m increases, the optimum variational state approaches the exact one systematically. In addition, the MPS can handle infinite system size directly if we suppose the spatial homogeneity of the MPS as in the iTEBD. As a merit of the spatially uniform MPS or iMPS, there are no boundary effects, which always appear in the DMRG.

In the zigzag chain,[1–8] the helical magnetic order with incommensurate period is known to be a solution of the classical vector spin Heisenberg model, which is valid in the large spin limit ($S \gg 1$). The incommensurate properties appear due to the geometrical frustration. To deal with quantum fluctuations, one can use the MPS. However, the spatially uniform MPS with a finite dimension cannot express the helical magnetic order because its local magnetic moment becomes spatially uniform. On the other hand, the DMRG can deal with a spatially inhomogeneous magnetic order, but the boundary affects the incommensurate period of the order.

In this study, we propose a simple incommensurate (IC) MPS with incommensurate periodicity applying spin rotation operators[17] to the spatially uniform MPS. This IC-MPS is understood naturally as a quantum generalization of the classical vector spin analysis. This framework is independent of the type of numerical optimization process, and it is applicable for various variational methods based on finite-dimensional MPSs: DMRG,[9–11] the wave function predictions based on the product wave-function renormalization group (PWFRG) method,[18–22] the tensor product state (TPS),[23,24] the projected entangled pair state (PEPS),[25] iTEBD,[13] the infinite PEPS (iPEPS),[26] the tree tensor network (TTN) state,[27] the multiscale entanglement renormalization ansatz (MERA) state,[28] and so on. To demonstrate our lightweight modification for the uniform MPS with a small dimension of matrices m, the modified Powell method[29] is used as a general purpose optimization method in this paper.

A pitch angle which determines an incommensurate period is a variational parameter in our approach. The pitch angle plays an important role in the optimization of the variational energy. This is caused by the finite-m effect because any state can be expressed by the MPS with infinite m. However, in the analysis of a quantum effect starting from the classical vector spin model our approach shows a fast convergence with respect to m, and a result obtained with a tiny m is consistent with IC spin-spin correlation properties.[1,3]

The spatial periodicity and translational symmetry are recent hot topics for the MPS and its generalization.[30–34] Our previous study[34] showed that in the spatially uniform MPS the translational symmetry breaking appeared in the principal eigenvalues of its transfer matrix; that is, the degeneracy of eigenvalues was consistent with the ground-state periodicity. This means that we need a large dimension of matrices for the spatially uniform MPS with one-site periodicity to express a magnetic ordered state with p-site commensurate periodicity. To reduce computational memory without losing the numerical accuracy, p-site periodic MPS was effective.[34] However, as shown in this study, we succeed in reducing more computational memory using the IC-MPS.

This paper is organized as follows. In Sec. II, we review the interaction-round-a-face (IRF)/vertex-type MPS[34–36] and propose the IC-MPS. The MFA limit of the IC-MPS is discussed in Sec. III, where we show that the optimum vertex-type IC-MPS with $m = 1$ in the $S = 1/2$ Heisenberg chain is equivalent to the state from the MFA. In Sec. IV, observing the m dependence of local magnetization in the $S = 1/2$ Heisenberg chain, we confirm the IC-MPS takes into account the quantum fluctuations gradually by increasing m. In the same section, the effectiveness of the IC-MPS is demonstrated in the magnetization curve of the $S = 1/2$ Heisenberg chain and the $S = 1/2$ FM-AFM zigzag chain under uniform magnetic field. Then, we discuss the reduced

computational cost by applying the spin rotation in the $S = 1/2$ Heisenberg chain and the commensurate-incommensurate (C-IC) change with respect to the spin-spin correlation in the zigzag chain.[1–3,7,8]

II. MATRIX PRODUCT STATE WITH AN INCOMMENSURATE PERIOD

Let us recall the IRF/vertex-type MPS.[34–36] An IRF-type MPS with N sites is

$$|\Psi\rangle = \sum_{\sigma} \mathrm{Tr}\left[A_0^{\sigma_N \sigma_1} \prod_{i=1}^{N-1} A_i^{\sigma_i \sigma_{i+1}} \right] |\sigma\rangle, \tag{1}$$

where σ_i is the index of spin at the ith site and $\sigma = \sigma_1 \cdots \sigma_N$. The variables $A_0^{\sigma_N \sigma_1}$ and $A_i^{\sigma_i \sigma_{i+1}}$ are $m \times m$ square complex matrices. The matrix $A_0^{\sigma_N \sigma_1}$ is called the boundary matrix.[14,15,34,37] A vertex-type MPS is represented under the constraints $A_0^{\sigma_N \sigma_1} = A^{\sigma_N} A_0$ and $A_i^{\sigma_i \sigma_{i+1}} = A_i^{\sigma_i}$. To handle the thermodynamic limit ($N \to \infty$), hereafter, we treat a uniform MPS, namely, $A_i^{\sigma_i \sigma_{i+1}} = A^{\sigma_i \sigma_{i+1}}$. As in our previous study,[34] one can treat the p-site periodic MPS.

To construct an IC-MPS, we use a spin-rotational operator at each ith site:[17]

$$\hat{R}_i(\boldsymbol{n}_i, Q_i) = \exp(-\mathbf{i} Q_i \hat{\boldsymbol{s}}_i \cdot \boldsymbol{n}_i), \tag{2}$$

where $\mathbf{i}$ is a unit of a pure imaginary number and $\hat{\boldsymbol{s}}_i$ is the local spin operator. The unit vector of the rotational axis and the angle at each site are represented by $\boldsymbol{n}_i$ and Q_i, respectively. In this paper, we limit ourselves to the simple case of $\boldsymbol{n}_i = \boldsymbol{n}$ and $Q_i = iQ$.

Then, the IC-MPS is given by

$$|\Psi, \boldsymbol{n}, Q\rangle = \left[\prod_i \hat{R}_i(\boldsymbol{n}, iQ) \right] |\Psi\rangle = \hat{R}_{\mathrm{tot}}(\boldsymbol{n}, Q) |\Psi\rangle. \tag{3}$$

A schematic picture of the wave function of IC-MPS is depicted in Fig. 1, where R_i is a matrix representation of the operator $\hat{R}_i$.

The variational energy for a Hamiltonian $\hat{H}$ is given by $e(\Psi, \boldsymbol{n}, Q) = \lim_{N\to\infty} E(\Psi, \boldsymbol{n}, Q)/N$, with

$$\begin{aligned} E(\Psi, \boldsymbol{n}, Q) &= \langle \Psi, \boldsymbol{n}, Q | \hat{H} | \Psi, \boldsymbol{n}, Q \rangle / \langle \Psi, \boldsymbol{n}, Q | \Psi, \boldsymbol{n}, Q \rangle \\ &= \langle \Psi | \hat{H}(\boldsymbol{n}, Q) | \Psi \rangle / \langle \Psi | \Psi \rangle, \end{aligned} \tag{4}$$

$$\hat{H}(\boldsymbol{n}, Q) = \hat{R}_{\mathrm{tot}}^{\dagger}(\boldsymbol{n}, Q) \hat{H} \hat{R}_{\mathrm{tot}}(\boldsymbol{n}, Q), \tag{5}$$

where $\hat{H}(\boldsymbol{n}, Q)$ is the spin-rotated Hamiltonian. Hereafter, we just consider $\hat{H}(\boldsymbol{n}, Q)$.

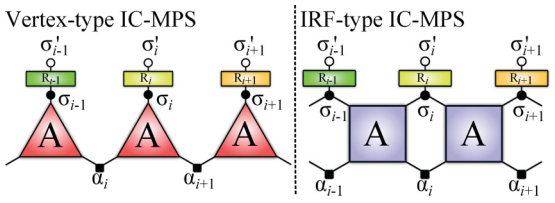

FIG. 1. (Color online) Graphical representations of vertex-type IC-MPS and IRF-type IC-MPS. Solid circles and small solid squares indicate contraction with respect to the local spin bases σ_i and the local artificial bases α_i of the matrix A, respectively.

For general $\boldsymbol{n}_i$ and Q_i, the useful formulae of the spin-rotated operator are summarized below. The rotated local spin operator in general spin S is given by

$$\hat{\boldsymbol{s}}_i(\boldsymbol{n}_i, Q_i) = \hat{R}_i^{\dagger}(\boldsymbol{n}_i, Q_i) \hat{\boldsymbol{s}}_i \hat{R}_i(\boldsymbol{n}_i, Q_i) = \mathbf{D}(\boldsymbol{n}_i, Q_i) \hat{\boldsymbol{s}}_i, \tag{6}$$

where the three-dimensional matrix $\mathbf{D}(\boldsymbol{n}_i, Q_i)$ is given by

$$\begin{aligned} [\mathbf{D}(\boldsymbol{v}, q)]_{\eta\eta'} &= v_\eta v_{\eta'} + (\delta_{\eta\eta'} - v_\eta v_{\eta'}) \cos q \\ &\quad - \sin q \sum_{\eta''} \epsilon_{\eta\eta'\eta''} v_{\eta''} \end{aligned} \tag{7}$$

for the unit vector $\boldsymbol{v}$. The symbols $\delta_{\eta\eta'}$ and $\epsilon_{\eta\eta'\eta''}$ represent the Kronecker delta and the Levi-Civita symbol, respectively, where $\eta = x, y, z$. From Eq. (7), we can immediately obtain the relation $\mathbf{D}(\boldsymbol{n}_i, Q_i)^{\mathrm{t}} = \mathbf{D}(\boldsymbol{n}_i, -Q_i)$.

For the simple case of $\boldsymbol{n}_i = \boldsymbol{n}$ and $Q_i = iQ$, one can prove the following equation:

$$\hat{\boldsymbol{s}}_i(\boldsymbol{n}, iQ) \cdot \hat{\boldsymbol{s}}_{i+\ell}(\boldsymbol{n}, iQ + \ell Q) = \hat{\boldsymbol{s}}_i \cdot \hat{\boldsymbol{s}}_{i+\ell}(\boldsymbol{n}, \ell Q). \tag{8}$$

The vanishing of the position dependence simplifies the calculation of the Heisenberg Hamiltonian. For the $S = 1/2$ Heisenberg chain defined by

$$\hat{H}_1 = \sum_i \hat{\boldsymbol{s}}_i \cdot \hat{\boldsymbol{s}}_{i+1}, \tag{9}$$

the spin-rotated Hamiltonian $\hat{H}_1(\boldsymbol{n}, Q)$ is written as

$$\hat{H}_1(\boldsymbol{n}, Q) = \sum_i \hat{\boldsymbol{s}}_i \cdot \hat{\boldsymbol{s}}_{i+1}(\boldsymbol{n}, Q) = \sum_i \hat{h}_i(\boldsymbol{n}, Q). \tag{10}$$

This Hamiltonian has translational symmetry. Next, we apply the same uniform MPS used in the previous study.[34] If the artificial translational-symmetry breaking does not occur, we can neglect the boundary matrix, and the local energy $e_i = \langle \Psi | \hat{h}_i(\boldsymbol{n}, Q) | \Psi \rangle$ becomes independent of position i in the thermodynamic limit. The translational symmetry of the spin-rotated Hamiltonian is recovered even for the zigzag and bilinear-biquadratic Heisenberg chain for general spin S.

It should be noted that we can deal with the case where the spin-rotated Hamiltonian does not have translational symmetry. In this case, we can calculate the variational energy by using the translational symmetry of the MPS $|\Psi\rangle$ because the position dependence of the local energy e_i can be expanded as

$$e_i = e^{(0)} + \sum_{k \neq 0} e^{(k)} \exp(\mathbf{i} i k Q) \tag{11}$$

and only $e^{(0)}$ gives a nonzero contribution after taking the summation $\sum_i e_i$ if Q is not commensurate. For commensurate Q, we must consider the contribution from $e^{(k)}$ for $k \neq 0$. Of course, one can treat more general position-dependent rotations, for example, $Q_{2i} = 2iQ_{\mathrm{a}}$ and $Q_{2i+1} = (2i+1)Q_{\mathrm{b}}$, where the expansion as in Eq. (11) becomes more complex, namely, $e_i = e^{(0,0)} + \sum_{(k_{\mathrm{a}}, k_{\mathrm{b}}) \neq (0,0)} e^{(k_{\mathrm{a}}, k_{\mathrm{b}})} \exp[\mathbf{i} i (k_{\mathrm{a}} Q_{\mathrm{a}} + k_{\mathrm{b}} Q_{\mathrm{b}})]$.

III. MEAN-FIELD APPROXIMATION LIMIT

We derive the mean-field limit of this method, which is realized by the vertex-type IC-MPS with $m = 1$. In this limit,

we can neglect the boundary A_0, which has only two trivial roles: normalization and phase factor. Then, the MPS becomes a direct product state $|\Psi\rangle = \sum_\sigma \prod_i (A^{\sigma_i}|\sigma_i\rangle)$, expressed by two complex variables, $A^\uparrow$ and $A^\downarrow$, in $S = 1/2$ systems. As a normalization, we assume $\sum_{\sigma_i} |A^{\sigma_i}|^2 = 1$.

To show that the mean-field limit corresponds to the classical vector spin model, we consider the Heisenberg Hamiltonian H_1. The variational energy is given by

$$e(\Psi, \boldsymbol{n}, Q) = \boldsymbol{M} \cdot [\mathbf{D}(\boldsymbol{n}, Q)\boldsymbol{M}], \tag{12}$$

with an expectation value of local magnetic moment $\boldsymbol{M} = \sum_{\sigma,\sigma'} A^{\sigma *} A^{\sigma'} \langle\sigma|\hat{\boldsymbol{s}}|\sigma'\rangle$. The local magnetization is obtained wit $|\boldsymbol{M}| = \sqrt{\boldsymbol{M}^2}$. After the optimization for fixed Q, one can obtain

$$e(Q) = \min_{\Psi, \boldsymbol{n}} e(\Psi, \boldsymbol{n}, Q) = \cos Q/4. \tag{13}$$

Then, the optimization of $e(Q)$ gives the Néel-type solution $Q = \pi$. We stress again that this energy gain of $e(Q) - e(0)$ is due to finite m because any state can be expressed by the uniform $(p = 1, Q = 0)$ MPS accurately if we have a large enough dimension m for the MPS. This finite dimensionality also causes $|\boldsymbol{M}| = 1/2$, which is always proved for any state in the mean-field limit, while it is known that the exact ground state does not have magnetization at zero magnetic field. In this sense, the mean-field limit corresponds to the classical vector spin model. In fact, as shown in Sec. IV, when we increase m to express quantum fluctuations or entanglement, the local magnetization $|\boldsymbol{M}|$ obtained after the optimization decreases and approaches the exact value.

IV. NUMERICAL RESULT AND DISCUSSION

Before showing results, we summarize the details of our numerical calculation. We prepare the m-dimensional complex matrix $A^{\sigma_i,\sigma_{i+1}}$ for the IRF-type uniform MPS. The rotational axis $\boldsymbol{n}$ is fixed as $(0,0,1)$ to conserve the translational symmetry of the rotated uniaxial Hamiltonian with the longitudinal magnetic field H_z applied on the z axis. The pitch Q and $A^{\sigma_i,\sigma_{i+1}}$ are optimized so that the variational energy e for a given Hamiltonian $\hat{H}$ becomes the minimum by using the modified Powell method.[29] The number of optimization parameters in the IRF-type IC-MPS under a fixed rotational axis is $2d^2m^2 + 1$, where the coefficient 2 comes from using complex numbers and d is the degrees of freedom (DOF) of local spin, namely, 2 in this work. The term $+1$ means the DOF of the wave number Q. In the optimization, 10–2000 initial states are prepared and optimized in each Hamiltonian parameter to avoid obtaining a local minimum.

The MPS gradually takes into account the quantum fluctuations of the local magnetic moment in the $S = 1/2$ Heisenberg chain with increasing m, as shown in Fig. 2. The rotational angle $Q = \pi$ is obtained after the optimization. The energy error ΔE means the difference between optimized variational energies as function of m and the exact energy $-\ln 2 + 1/4$.[38] The energy error and the local magnetization $|\boldsymbol{M}|$ are monotonically decreasing with respect to m. We confirm that the IRF-type MPS can deal with nonzero quantum fluctuations even if $m = 1$, while the vertex-type MPS with

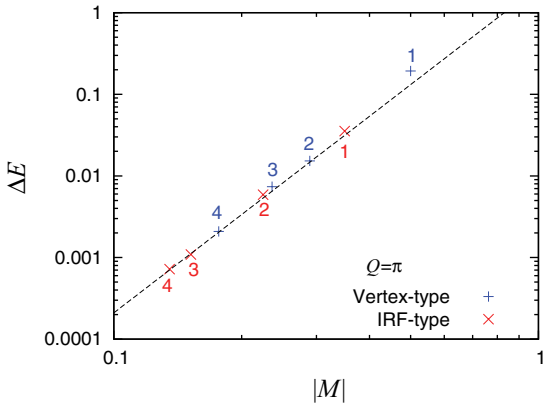

FIG. 2. (Color online) Energy error ΔE as a function of local magnetization $|\boldsymbol{M}|$ in the $S = 1/2$ Heisenberg chain $\hat{H}_1$. The number near each symbol indicates the matrix dimension m. The dashed line is guide for the eye, showing the power-law decay of $\Delta E \propto |\boldsymbol{M}|^4$.

$m = 1$ gives the mean-field result. This is an advantage of using an IRF-type MPS.

The magnetization M_z in the $S = 1/2$ Heisenberg chain with the magnetic field H_z is shown in Fig. 3. As reference data, we show the exact result for $S = 1/2$ from the Bethe ansatz[38] and the result from two-site modulated MPS, called $p = 2$, $Q = 0$, in our previous study.[34] While the mean-field result fails to obtain the correct criticality near the fully saturated point, results for $m = 3$, which is not a very large dimension, show enough accuracy.

This increasing of m leads to a great improvement in the accuracy of estimating the magnetization curve. The relative error of the magnetization curve from the IC-MPS with $m = 3$ in Fig. 3 is smaller than 3%, even though the error of local magnetization $|\boldsymbol{M}|$ is of the order of that from the MFA, as shown in Fig. 2; that is, the absolute error of M_z in Fig. 3 is less than 0.001, even though the error of $|\boldsymbol{M}|$ in Fig. 2 is about 0.1.

Moreover, in the cases of both $m = 1$ and $m = 3$, the data from IC-MPS with $Q = \pi$ agree with those of the $p = 2, Q = 0$ MPS. This means that the number of optimization parameter is reduced by 50% compared to our previous study.

How the rotational pitch $Q = \pi$ is stabilized by the energy gain, $e(Q) - e(0)$, is shown in Fig. 4, which clearly shows

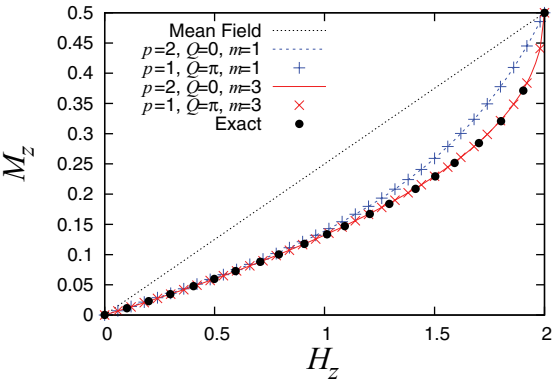

FIG. 3. (Color online) Magnetization M_z curve as a function of uniform magnetic field H_z in the $S = 1/2$ Heisenberg chain $\hat{H}_1$.

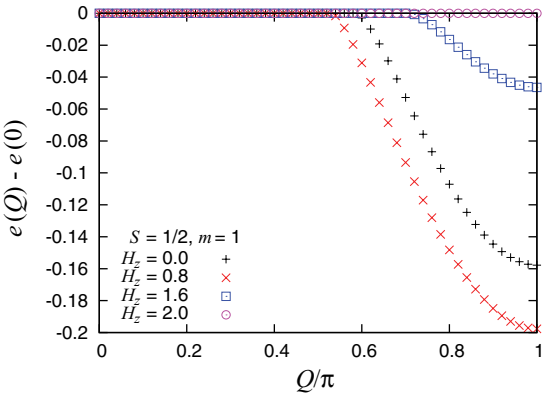

FIG. 4. (Color online) Rotational parameter Q dependence of the variational energy in the $S = 1/2$ Heisenberg chain $\hat{H}_1$.

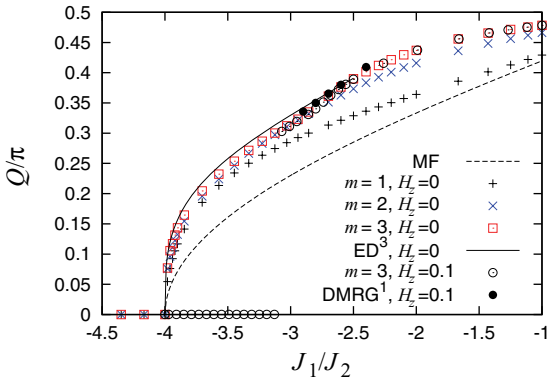

FIG. 5. (Color online) Rotational parameter Q as a function of J_1/J_2 in the zigzag chain $\hat{H}_2$.

that the variational energy becomes minimum at $Q = \pi$ for any magnetic field except for $H_z = 2.0$ in the fully saturated ferromagnetic region. Compared with $e(Q) = \cos Q/4$ for $H_z = 0$ in the mean-field limit, there is a flat energy region in the small Q region for $H_z = 0$. In the flat region, we confirm the state is a superposition of the Néel state, namely, the linear combination of $|\uparrow\downarrow\uparrow\cdots\rangle$ and $|\downarrow\uparrow\downarrow\cdots\rangle$.[34] This state is invariant with respect to the spin rotation along the z axis. The origin of the flat region is the quantum fluctuations of the Néel state. This quantum fluctuations can be expressed by the IRF even for $m = 1$.

Finally, we discuss the periodicity change appearing in the $S = 1/2$ FM-AFM ($J_1 < 0$ and $J_2 > 0$) zigzag Heisenberg chain with uniform longitudinal magnetic field,

$$\hat{H}_2 = \sum_i \left(\sum_{k=1,2} J_k \hat{\mathbf{s}}_i \cdot \hat{\mathbf{s}}_{i+k} - H_z \hat{s}_i^z \right). \tag{14}$$

The longitudinal magnetic field H_z is taken as 0 and 0.1 in this analysis. At $H_z = 0$, there is a C-IC change at $J_1/J_2 = -4$. The commensurate state for $J_1/J_2 < -4$ is a ferromagnetic state, while the characterization of the ground state for $J_1/J_2 > -4$ is a difficult task. A recent study[2] pointed out that the ground state for $J_1/J_2 > -4$ is the Haldane-dimer phase, which is characterized by a generalized string order parameter, where ordinal spin-spin correlations behave incommensurately.[3] This incommensurate behavior is also found in the vector chiral (VC) phase for nonzero magnetic fields.[1]

To demonstrate our approach for the C-IC change, the optimized pitch Q is calculated for this frustrated Hamiltonian $\hat{H}_2$, as shown in Fig. 5. In Fig. 5 there are three kinds of the reference data. First, the dashed line is the result of the mean-field approximation, $Q = \arccos(-J_1/4J_2)$. Second, the solid line is the fitting line for the location of the maximum of the zero-field spin structure factor with the ED,[3] where $Q \propto (J2 - 1/4)^{0.29}$. Finally, the solid circles are the result of the DMRG at $M_z = 0.05$ in the VC phase.[1] For $H_z = 0$, the pitch Q approaches $\pi/2$ with increasing J_1/J_2 more rapidly than that of the mean-field approximation, because the MPSs with larger m can take into account more quantum fluctuations than the MPS with smaller m. On the other hand, the C-IC change point is completely converged at $J_1/J_2 = -4$. We find the pitch in $m = 3$ is comparable to the result from ED[3] in $J1/J2 \leqslant -2.5$. Around the transition point, the pitch is well converged with respect to m on this scale. The m dependence gradually becomes large with increasing J_1/J_2, where the frustration due to J_2 also gradually becomes large.

For $H_z = 0.1$, the pitch Q depicted by the open circle in Fig. 5 has a jump around $J_1/J_2 = -3.1$, which is very close to the SDW$_3$-VC phase transition point.[1] Unfortunately, the pitch Q for small m fails to capture the two kinds of spin-density wave (SDW$_2$ and SDW$_3$)[1] states, where the ferromagnetic-SDW$_3$ phase transition occurs at $J_1/J_2 \sim -3.3$ and the VC-SDW$_2$ phase transition occurs at $J_1/J_2 \sim -2$.[1] At the same time, the characterization of the ground state at $H_z = 0$ is difficult for our method at this stage. Nevertheless, a notable point is that the incommensurate pitch Q of the IC-MPS for the VC phase in $J_1/J_2 > -3.1$ shows reasonable agreement with the DMRG result. For $J_1/J_2 > -3.1$, Q of the IC-MPS is nearly independent of H_z, which is also consistent with the DMRG analysis.[1]

V. SUMMARY

In summary, we introduced the IRF-type MPS with the incommensurate pitch parameter Q and the rotational axis $\boldsymbol{n}$ as a generalization of the uniform MPS, which can be used for various variational methods based on the MPS. Two parameters, Q and $\boldsymbol{n}$, allow us to evaluate an incommensurability of the spin chain in the thermodynamic limit directly. Our approach with a small dimension of matrices is connected to the classical vector spin Heisenberg model, which is valid in the large spin limit ($S \gg 1$). For the exact ground state, the helical magnetic order obtained in the classical limit is expected to be destroyed by quantum fluctuations in the quantum limit $S = 1/2$. However, we emphasize the quantum effects on some quantities are rapidly converged with respect to the matrix dimension. Our approach opens a way for a lightweight analysis based on the classical vector spin model to include quantum fluctuations. Using this approach, one can treat translational symmetry-broken states, such as the helical magnetic order, in the thermodynamic limit, which cannot be handled by known iMPS with translational symmetry.

We demonstrated the efficiency of this IRF-type IC-MPS in two types of Hamiltonians: (i) the magnetization in the $S = 1/2$ antiferromagnetic Heisenberg chain under uniform magnetic field and (ii) the C-IC change in the $S = 1/2$

FM-AFM Heisenberg zigzag chain under uniform magnetic field. In the former Hamiltonian, we have succeeded in obtaining the same result as a two-site modulated MPS. This means a 50% reduction in the number of optimization parameters. In the latter Hamiltonian, we have succeeded in detecting the C-IC change of the correlation properties with increasing m. The pitch Q near the C-IC transition point is immediately converged with respect to m and shows a reasonable agreement with the ED study[3] and the DMRG study,[1] despite the small m.

On the other hand, the sufficiently converged Q is not obtained around the strongly frustrated region, namely, $|J_1| \sim J_2$. To discuss the details of Q, an analysis with larger m is necessary. For this problem, we can apply other optimization methods using the Trotter decomposition,[13] the matrix product operator,[39] and the time-dependent variational principle[40] to update the MPS under given Q_i and $\boldsymbol{n}_i$. We stress again that the framework of IC-MPS is independent of the type of numerical optimization process. In this paper, the modified Powell method was chosen as an optimization method because it is a general-purpose method and all parameters are optimized easily. The modified Powell method is enough to clarify the effectiveness of our lightweight modification but becomes a bottleneck when we increase m. To study larger m, the convergence properties and numerical efficiencies of these updating methods should be discussed. This problem should be addressed in future work.

Another future issue is to change the constraint of the rotational axis and pitch parameter in order to represent the magnetization plateau state or the SDW state, for example, $\boldsymbol{n}_i = \boldsymbol{n}_{\mathrm{mod}[i,p]}$ and $Q_i = Q_{\mathrm{mod}[i,p]}$. This method uses the spin-rotational operator, which maps the classical helical state to the fully saturated ferromagnetic state. The uniform direct product state including the fully saturated ferromagnetic state can always be described by the uniform MPS with $m = 1$. A generalization of this method is to find another kind of spin-rotational operator which maps the ground state to the uniform direct product state. The role of this operation is similar to disentanglers in the MERA.[28] In this sense, it is interesting to consider the valence bond solid state, which cannot be rotated by the spin-rotational operators[17] and is known to have Kennedy-Tasaki transformation, which converts the string order to the ferromagnetic order as a global topological disentangler.[41,42]

In general, the classical magnetic order can be found easily in higher-dimensional systems. In this case, the spin rotation becomes effective. Moreover, in higher-dimensional systems, the dimension of the matrix/tensor is restricted due to the computational resources. Therefore a small-m analysis based on our approach is an interesting approach for the incommensurate TPS for two-dimensional quantum spin systems, which is another issue for the future. In addition to TPS, our approach can be applied to various methods.

ACKNOWLEDGMENTS

We acknowledge discussions with S. Miyahara. This work was supported in part by a Grant-in-Aid for JSPS Fellows and Grant-in-Aid No. 20740214, Global COE Program (Core Research and Engineering of Advanced Materials-Interdisciplinary Education Center for Materials Science), from the Ministry of Education, Culture, Sports, Science and Technology of Japan.

*hueda@riken.jp
†maru@mp.es.osaka-u.ac.jp

[1] T. Hikihara, L. Kecke, T. Momoi, and A. Furusaki, Phys. Rev. B **78**, 144404 (2008).
[2] M. Sato, S. Furukawa, S. Onoda, and A. Furusaki, Mod. Phys. Lett. B **25**, 901 (2011).
[3] J. Sudan, A. Lüscher, and A. M. Läuchli, Phys. Rev. B **80**, 140402 (2009).
[4] F. Heidrich-Meisner, A. Honecker, and T. Vekua, Phys. Rev. B **74**, 020403 (2006).
[5] L. Kecke, T. Momoi, and A. Furusaki, Phys. Rev. B **76**, 060407 (2007).
[6] T. Vekua, A. Honecker, H.-J. Mikeska, and F. Heidrich-Meisner, Phys. Rev. B **76**, 174420 (2007).
[7] K. Okunishi, J. Phys. Soc. Jpn. **77**, 114004 (2008).
[8] I. P. McCulloch, R. Kube, M. Kurz, A. Kleine, U. Schollwöck, and A. K. Kolezhuk, Phys. Rev. B **77**, 094404 (2008).
[9] S. R. White, Phys. Rev. Lett. **69**, 2863 (1992); Phys. Rev. B **48**, 10345 (1993).
[10] I. Peschel, X. Wang, M. Kaulke, and K. Hallberg, *Density-Matrix Renormalization: A New Numerical Method in Physics* (Springer, Berlin, 1999).
[11] U. Schollwöck, Rev. Mod. Phys. **77**, 259 (2005).
[12] K. A. Hallberg, Adv. Phys. **55**, 477 (2006).
[13] G. Vidal, Phys. Rev. Lett. **98**, 070201 (2007).
[14] S. Östlund and S. Rommer, Phys. Rev. Lett. **75**, 3537 (1995).
[15] S. Rommer and S. Östlund, Phys. Rev. B **55**, 2164 (1997).
[16] U. Schollwöck, Ann. Phys. (NY) **326**, 96 (2011).
[17] E. Lieb, T. Schultz, and D. Mattis, Ann. Phys. (NY) **16**, 407 (1961).
[18] T. Nishino and K. Okunishi, J. Phys. Soc. Jpn. **64**, 4084 (1995).
[19] K. Ueda, T. Nishino, K. Okunishi, Y. Hieida, R. Derian, and A. Gendiar, J. Phys. Soc. Jpn. **75**, 014003 (2006).
[20] H. Ueda, T. Nishino, and K. Kusakabe, J. Phys. Soc. Jpn. **77**, 114002 (2008).
[21] I. P. McCulloch, arXiv:0804.2509.
[22] H. Ueda, A. Gendiar, and T. Nishino, J. Phys. Soc. Jpn. **79**, 044001 (2010).
[23] H. Niggemann, A. Klumper, and J. Zittartz, Z. Phys. B **104** 103 (1997); Eur. Phys. J. B **13** 15 (2000).
[24] M. A. Martin-Delgado, M. Roncaglia, and G. Sierra, Phys. Rev. B **64**, 075117 (2001).
[25] F. Verstraete, M. M. Wolf, D. Perez-Garcia, and J. I. Cirac, Phys. Rev. Lett. **96**, 220601 (2006).
[26] J. Jordan, R. Orús, G. Vidal, F. Verstraete, and J. I. Cirac, Phys. Rev. Lett. **101**, 250602 (2008).

[27]Y.-Y. Shi, L.-M. Duan, and G. Vidal, Phys. Rev. A **74**, 022320 (2006).
[28]G. Vidal, Phys. Rev. Lett. **101**, 110501 (2008).
[29]W. H. Press, S. A. Teukolsky, W. T. Vetterling, and B. P. Flannery, *Numerical Recipes in Fortran 90* (Cambridge University Press, New York, 1996).
[30]C. Liu, L. Wang, A. W. Sandvik, Y.-C. Su, and Y.-J. Kao, Phys. Rev. B **82**, 060410 (2010).
[31]B. Pirvu, F. Verstraete, and G. Vidal, Phys. Rev. B **83**, 125104 (2011).
[32]J. Haegeman, B. Pirvu, D. J. Weir, J. I. Cirac, T. J. Osborne, H. Verschelde, and F. Verstraete, Phys. Rev. B **85**, 100408(R) (2012).
[33]B. Pirvu, J. Haegeman, and F. Verstraete, Phys. Rev. B **85**, 035130 (2012).
[34]H. Ueda, I. Maruyama, and K. Okunishi, J. Phys. Soc. Jpn. **80**, 023001 (2011).
[35]R. J. Baxter, *Exactly Solved Models in Statistical Mechanics* (Academic, London, 1982).
[36]G. Sierra and T. Nishino, Nucl. Phys. B **495**, 505 (1997).
[37]I. Maruyama and H. Katsura, J. Phys. Soc. Jpn. **79**, 073002 (2010).
[38]M. Takahashi, *Thermodynamics of One-Dimensional Solvable Models* (Cambridge University Press, Cambridge, 1999).
[39]B. Pirvu, V. Murg, J. I. Cirac, and F. Verstraete, New J. Phys. **12**, 025012 (2010).
[40]J. Haegeman, J. I. Cirac, T. J. Osborne, I. Pižorn, H. Verschelde, and F. Verstraete, Phys. Rev. Lett. **107**, 070601 (2011).
[41]K. Okunishi, Phys. Rev. B **83**, 104411 (2011).
[42]I. Maruyama, arXiv:1109.4202.